Eur Biophys J (1986) 13:157–173

European Biophysics Journal

The superstructure of chromatin and its condensation mechanism

I. Synchrotron radiation X-ray scattering results

J. Bordas[1], L. Perez-Grau[2]*, M. H. J. Koch[2], M. C. Vega[2], and C. Nave[1]

[1] MRC/SERC Biology Support Laboratory, Daresbury Laboratory, Warrington WA4 4AD, United Kingdom
[2] European Molecular Biology Laboratory, c/o DESY, Notkestrasse 85, D-2000 Hamburg 52, Federal Republic of Germany

Received April 10, 1985/ Accepted in revised form August 28, 1985

Abstract. Synchroton radiation X-ray scattering experiments have been performed on chicken erythrocyte chromatin fibres over a wide range of ionic conditions and on various states of the fibres (i.e. "native" in solution, in gels and in whole nuclei; chromatin depleted of the H1 (H5) histones and chromatin with bound ethidium bromide).

A correlation between the results obtained with the various chromatin preparations provides evidence for a model according to which at low ionic strength the chromatin fibre already possesses a helical superstructure, with a diameter comparable to that of condensed chromatin, held together by the H1 (H5) histone. The most significant structural modification undergone upon an increase of the ionic strength is a reduction of the helix pitch, this leads to condensation in a manner similar to the folding of an accordion. The details of this process depend on whether monovalent or divalent cations are used to raise the ionic strength, the latter producing a much higher degree of condensation. Measurements of the relative increase of the mass per unit length indicate that the most condensed state is a helical structure with a pitch around 3.0–4.0 nm.

In this paper we give a detailed presentation of the experimental evidence obtained from static and time-resolved scattering experiments, which led to this model.

Key words: Synchroton radiation, chromatin superstructure, chromatin condensation

1. Introduction

Many X-ray diffraction studies have shown that solutions or gels of chromatin are characterized by exhibiting broad diffraction rings at spacings of around 11, 5.5, 3.7, 2.7 and 2.1 nm (e.g. Wilkins et al. 1959; Luzatti and Nicolaieff 1959). These diffraction bands are also seen in a variety of isolated nuclei and living cells under physiological salt conditions (Langmore and Schutt 1980; Notbohm and Harbers 1981; Langmore and Paulson 1983; Paulson and Langmore 1983). X-ray and neutron scattering profiles from dilute solutions of mononucleosomes only exhibit a shoulder at 6 nm and diffraction rings at 3.7, 2.7 and 2.1 nm, whereas the 11 and 5.5 nm rings are not observed (Hjelm et al. 1977; Richards et al. 1977; Damaschun et al. 1980). On the basis of these findings it has been concluded that while the 3.7, 2.7 and 2.1 nm rings originate from the internal structure of the nucleosome, the 11 and 5.5 nm rings must be due to higher order packing of the nucleosomes in the chromatin fibres (Finch and Klug 1976).

The structural modification induced by an increase of ionic strength, and leading to the condensation of chromatin, has been characterized by a variety of techniques: electron microscopy (Thoma et al. 1979), neutron diffraction (Suau et al. 1979), analytical centrifugation (Butler and Thomas 1980; Thomas and Butler 1980; Bates et al. 1981; Fulmer and Bloomfield 1982) and light scattering measurements (Campbell et al. 1978; Fulmer and Bloomfield 1982). All these investigations indicated that further coiling or folding of the chromatin fibre takes place with increasing salt and/or divalent cation concentration.

Electric birefringence studies (Marion 1984), static (Campbell et al. 1978) and dynamic light scattering experiments (Shaw and Schmitz 1979; Marion et al. 1981) on oligonucleosomes suggest a model of open helices for uncondensed chromatin.

There is an incompatibility between these conclusions and earlier X-ray and neutron small angle scattering data (Sperling and Tardieu 1976; Suau

* *Present address*
Instituto de Biologia de Barcelona, Juan de la Cierva, C. Jorge Girona Salgado s/n, Barcelona, Spain

et al. 1979) which suggested that the structure of uncondensed chromatin in solution was consistent with a nucleofilament model in which the nucleosome subunits are densely packed in a linear array resembling a rod with near 10 nm diameter and without internal contrast.

In synchrotron radiation X-ray scattering experiments it is possible to achieve better angular resolution with higher statistical accuracy than in conventional cameras. Possibly because of this reason, recent experiments on solutions and gels of chicken erythrocyte chromatin provided evidence for the existence, even at very low ionic strength, of a preformed helical superstructure, thus reconciling the conflicting observations. This structure appears to be maintained by the H1 (H5) histones. The results also suggested a model which allows rapid condensation of the nucleofilaments at higher ionic strength by a reduction of the pitch of the uncondensed chromatin helix (Perez-Grau et al. 1984).

We present here further experimental evidence for this model. The results reported include: (A) Characterization of the X-ray scattering patterns from condensed and uncondensed chromatin fibres in solutions, gels and whole nuclei. (B) A study of the effects of progressively increasing ionic strength with monovalent or divalent cations. (C) A study of the effects of ethidium bromide on the solution scattering patterns of uncondensed chromatin. (D) A study of the effects due to the removal of the histone H1 (H5). (E) A study of the condensation kinetics in solutions and gels by time-resolved X-ray scattering.

2. Materials and methods

A. Preparation of chicken erythrocyte nuclei and chromatin fragments

Chicken erythrocyte nuclei were prepared as described by Olins et al. (1976). Samples of the final nuclear pellet in a buffer containing 10 m*M* NaCl, 3 m*M* $MgCl_2$, 10 m*M* *Tris*/HCl, 0.2 m*M* PMSF, pH 7.5 were used for X-ray scattering measurements directly or after adjustment of the ionic conditions to either: 150 m*M* NaCl, 10 m*M* *Tris*, 1 m*M* EDTA, 0.2 m*M* PMSF, pH 7.5 or 5 m*M* *Tris*, 1 m*M* EDTA, 0.2 m*M* PMSF, pH 7.5 by resuspension of the nuclei in 50 volumes of the required buffer and collection of the resulting condensed or lysed nuclei by centrifugation at 2,000 *g* for 10 min. Chromatin fragments were prepared by nuclease digestion or purified nuclei according to Noll et al. (1975). Nuclei were adjusted to 100 A_{260} units/ml in 150 m*M* NaCl, 10 m*M* *Tris*, 0.5 m*M* $CaCl_2$ and digested at 37 °C for 1 min with 75 units/ml of micrococcal nuclease (Sigma). The reaction was stopped by addition of EDTA to 2 m*M* and chilling on ice. The resulting nuclear pellet was lysed in 50 m*M* NaCl, 10 m*M* *Tris*, 1 m*M* EDTA and the insoluble material separated by centrifugation at 10,000 *g* for 15 min. From 30% to 50% of the initial amount of DNA was recovered as soluble chromatin fragments in the supernatant. After extensive dialysis against 5 m*M* *Tris*, 1 m*M* EDTA, 0.2 m*M* PMSF, pH 7.5 this material was diluted in dialysis buffer and used as the starting sample for the X-ray scattering measurements.

B. Preparation of H1 (H5) *depleted chromatin fragments*

Chromatin fragments were depleted of H5 histone by the method of Bolund and Johns (1973). Chromatin was dissolved in a buffer containing 0.65 m*M* NaCl, 10 m*M* *Tris*, 1 m*M* EDTA, 0.2 m*M* PMSF to give a final concentration of 1 mg DNA/ml (20 A_{260} units/ml). BioRad AG 50 W-X2, cation exchange resin, previously equilibrated with the buffer was added to the chromatin solutions at a ratio of 4 : 1 (v/v) and the mixture stirred for 1 h at 4 °C. The mixture was centrifuged at 3,000 *g* for 10 min and the supernatant extensively dialyzed against 5 m*M* *Tris*, 1 m*M* EDTA, 0.2 m*M* PMSF, pH 7.5. The removal of H5 was systematically checked before starting any set of measurements by polyacrylamide gel electrophoresis (PAGE). Results are illustrated in Fig. 1. For the X-ray scattering measurements, this solution of H5 depleted chromatin was concentrated to 3–5 mg DNA/ml by forced dialysis against the same low ionic strength dialysis buffer using a Sartorius membrane device.

C. Preparation of chromatin gels

Chromatin gels were prepared by concentrating chromatin solutions by forced dialysis using Sartorius membranes. The solution of chromatin was adjusted to the required ionic conditions and concentrated against a similar buffer until a homogeneous gel formed at the bottom of the dialysis tips. The process was carried out at 4 °C, and took from 6 to 8 h. All the solutions contained 0.2 m*M* PMSF as a protease inhibitor.

D. Analysis of the DNA *content of the chromatin fragments*

The size distribution of the chromatin fragments was determined by analysis of their DNA in agarose gels. DNA was extracted as described by Zamenhoff (1957) after digestion of the chromatin samples with 0.5 mg/ml proteinase K (Boehringer) in 0.2 m*M*

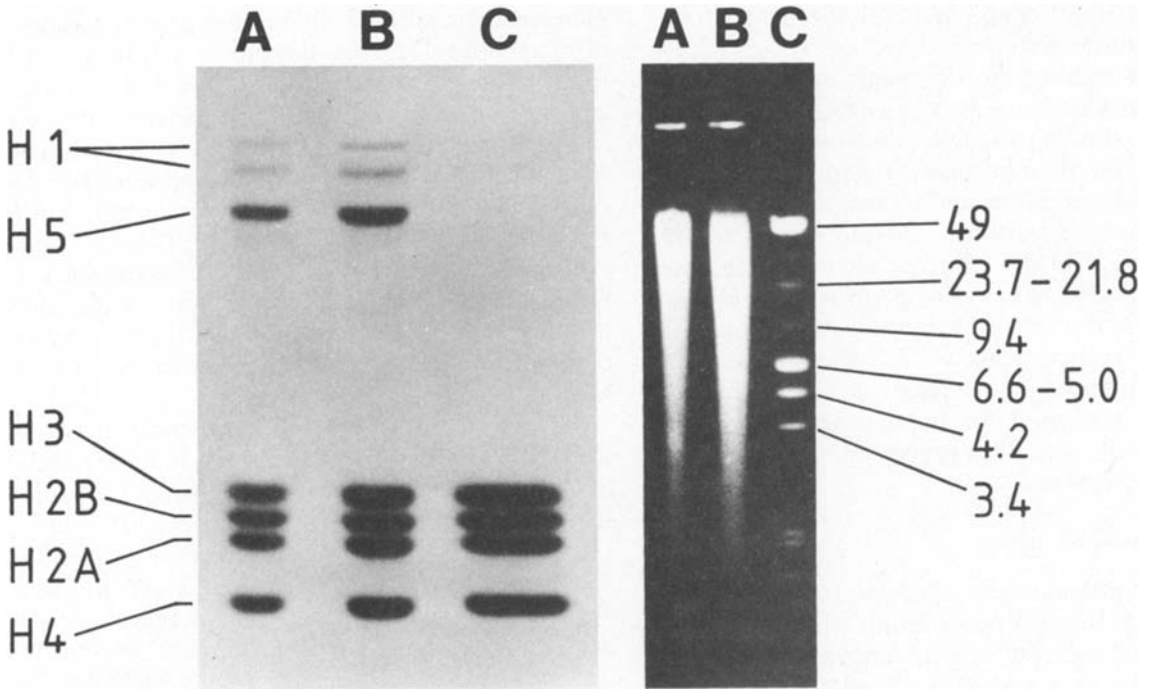

Fig. 1. *Left panel:* SDS-polyacrylamide gel of the histone complement of chromatin (*A*), chicken erythrocyte nuclei (*B*) and lysine-rich histone depleted chromatin (*C*). See Materials and methods for conditions. *Right panel:* DNA length distribution of two different preparations (*A* and *B*) determined by electrophoresis on a 0.8% agarose gel. The marker consisted of a mixture of lambda DNA, lambda Hind III digest and lambda Eco RI Hind III double digest. The lengths are given in kbases

NaCl, 10 m*M* EDTA, pH 8, 1% SDS. Electrophoresis was carried out in horizontal 0.8% agarose slab gels calibrated with a mixture of lambda-DNA, lambda Hind III digest and lambda Eco RI Hind III double digest, run in *Tris*/acetate buffer (Loening 1967). The fragment sizes were taken from Southern (1980). Typical results are illustrated in Fig. 1. Gels made before and after X-ray data collection were identical.

E. Analysis of the histone content of chromatin fragments

The protein content of samples used for X-ray scattering measurements was systematically checked by analysis in SDS/18% polyacrylamide gel electrophoresis according to Laemmli (1970). Typical results are illustrated in Fig. 1.

F. Measurement and processing of the scattering patterns

The scattering patterns were collected on the X-13 and X-33 cameras at the EMBL Outstation on the storage ring DORIS of the Deutsches Elektronen Synchrotron (DESY) at Hamburg (Hendrix et al. 1979; Koch and Bordas 1983) using the data acquisition systems described by Bordas et al. (1980); Boulin et al. (1982). The wavelength was 0.15 nm. The data were analyzed using a standard program package (Koch and Bendall 1981). The general procedures for data reduction (e.g. parasitic background removal, scattering vector calibration, detector response correction, etc. ...) were those described in Bordas et al. (1983). The data are presented in the usual $\log I(S) * S$ versus S ($S = 2\sin\Theta/\lambda$, where 2Θ is the scattering angle and λ the wavelength) plot for rod-like particles in solution and also in some cases, for easier visualization of the features, as plots of $\log I(S) * S^2$ versus S.

The radii of gyration of the cross-section were obtained from the slope of the very low angle part of the scattering curves in plots of $\log I(S) * S$ versus S^2, while the relative changes of mass per unit length were derived from the extrapolation of these curves to the origin (Kratky and Porod 1953; Luzatti 1960; Fedorov and Aleshin 1966).

Static X-ray scattering measurements were done on solutions of chromatin fragments at 3 to 7 mg DNA/ml. Screening measurements done at lower concentrations indicate that up to 7 mg DNA/ml the scattering pattern corresponds to a genuine solution pattern, and that interference effects are not detectable below 10 mg DNA/ml. Aliquots of the stock solution of chromatin fragments in 5 m*M* *Tris*, 1 m*M* EDTA, 0.2 m*M* PMSF, pH 7.5, were adjusted to the experimental ionic conditions of each mea-

surement by addition of 1 *M* NaCl, 0.1 *M* $MgCl_2$ or 25 m*M* ethidium bromide.

For time-resolved measurements, equal volumes of a chromatin solution at 10 mg DNA/ml and the appropriate double strength condensation buffer were mixed and data acquisition started simultaneously. The condensation buffers consisted of 5 m*M* *Tris* HCl, pH 7.5 adjusted to 200 m*M* NaCl, 6 m*M* $MgCl_2$, or 0.5 *M* EDTA. Buffer-buffer and chromatin-buffer dilution shots were performed to obtain background and reference spectra for the chromatin condensation experiments. A modified version of the X-ray stopped flow device described in Renner et al. (1983) was used for these experiments. The performance of the device prevented a time resolution better than 50 ms.

G. Nomenclature

In the description of experimental conditions the very low ionic strength preparations will be referred to throughout the text as chromatin-EDTA, while chromatin-NaCl (5 m*M* *Tris*, 50–150 m*M* NaCl, 1 m*M* EDTA, pH 7.5) and chromatin-$MgCl_2$ (5 m*M* *Tris*, 2–8 m*M* $MgCl_2$, 1 m*M* EDTA, pH 7.5) refer to high ionic strength conditions induced by salt or by Mg^{++} cations respectively. Since the solutions contain 1 m*M* EDTA all divalent cation concentrations required to obtain a given effect are systematically higher than in most other studies, e.g. Borochov et al. (1984) or Ausio et al. (1984).

3. Results

A. Characterization of the X-ray scattering patterns from the condensed and uncondensed states of "native" chromatin fibres in solution, whole nuclei and gels

A.1. Solutions. Typical X-ray scattering patterns from chromatin solutions are shown in Fig. 2. These patterns were obtained for solutions of chromatin at a concentration of 6.2 mg DNA/ml.

For concentrations below 30 m*M* NaCl/1 m*M* EDTA or 1 m*M* $MgCl_2$/1 m*M* EDTA, scattering patterns similar to those presented in Fig. 2a and d were always obtained. They can be regarded as representative of our preparations of uncondensed chromatin in dilute solutions (< 7 mg DNA/ml). They display a featureless decay of the scattered intensity for $S < 0.025\ nm^{-1}$ (the radius of gyration of the cross-section region) and a strong band near $0.05\ nm^{-1}$ which is a very characteristic marker for the degree of condensation of the fibres (throughout the text this band is referred to as the $0.05\ nm^{-1}$ band although its position and intensity vary slightly between preparations). Other characteristic features of chromatin-EDTA are the shoulder at $0.145\ nm^{-1}$, the high angle bands at 0.27, 0.365 and $0.47\ nm^{-1}$ and the trough at $0.22\ nm^{-1}$. The patterns displayed in Fig. 2b and c and Fig. 2e and f are characteristic of condensed chromatin in dilute solutions (i.e. for cation concentrations greater than 75 m*M* NaCl/1 m*M* EDTA or 2 m*M* $MgCl_2$/1 m*M* EDTA).

The traces in Fig. 2b and 2e correspond to typical patterns obtained at high, but not maximal, ionic strength. The traces shown in the figure were obtained by addition of divalent cations (5 m*M* Mg^{++}).

Similar patterns were obtained when the ionic strength was raised with NaCl (75–100 m*M*). Relative to the low ionic strength patterns, they exhibit a sharper decay in the intensities for $S < 0.035\ nm^{-1}$. The prominent $0.05\ nm^{-1}$ band has disappeared and a band appears at ca. $0.075\ nm^{-1}$. Simultaneously, a weak band near $0.045\ nm^{-1}$ and a prominent one near $0.16\ nm^{-1}$ have begun to develop. Beyond the trough at $0.22\ nm^{-1}$, the intensity has undergone an overall increase, roughly centered near $0.35\ nm^{-1}$. Superimposed on this background the 0.27, 0.365 and $0.47\ nm^{-1}$ bands can also be detected. The exact position and relative intensity of the bands at $S < 0.2\ nm^{-1}$ depend critically on the ionic conditions.

Figure 2c and f display the type of trace obtained when the ionic strength was raised to precipitation conditions by increasing the concentration of divalent cations. For the particular example shown in the figures the concentration of Mg^{++} was 8 m*M*. At this cation concentration the chromatin tended to precipitate slowly. Due to the speed of data acquisition characteristic of synchrotron radiation techniques (ca. 60 s) the patterns could be recorded before precipitation. The $0.04\ nm^{-1}$ band has disappeared and the 0.075 and $0.016\ nm^{-1}$ bands have shifted to about 0.09 and $0.17\ nm^{-1}$ and become much more prominent.

Although to a first approximation the patterns shown in Fig. 2 display the general trends associated with condensation of the chromatin fibres irrespective of the use of salt or Mg^{++}, there are significant differences between both cases, these will be discussed in Sect. D.

Also, although these trends were generally observed in all our experiments, the appearance and detailed behaviour of the various features were not only a function of the ionic strength but also of the chromatin concentration. For instance, near identical patterns are obtained at 6.2 mg DNA/ml – 5 m*M* $MgCl_2$ and at 3.5 mg DNA/ml – 3 m*M* $MgCl_2$, indicating that, from the point of view of condensation and eventual precipitation, the relevant factor is the

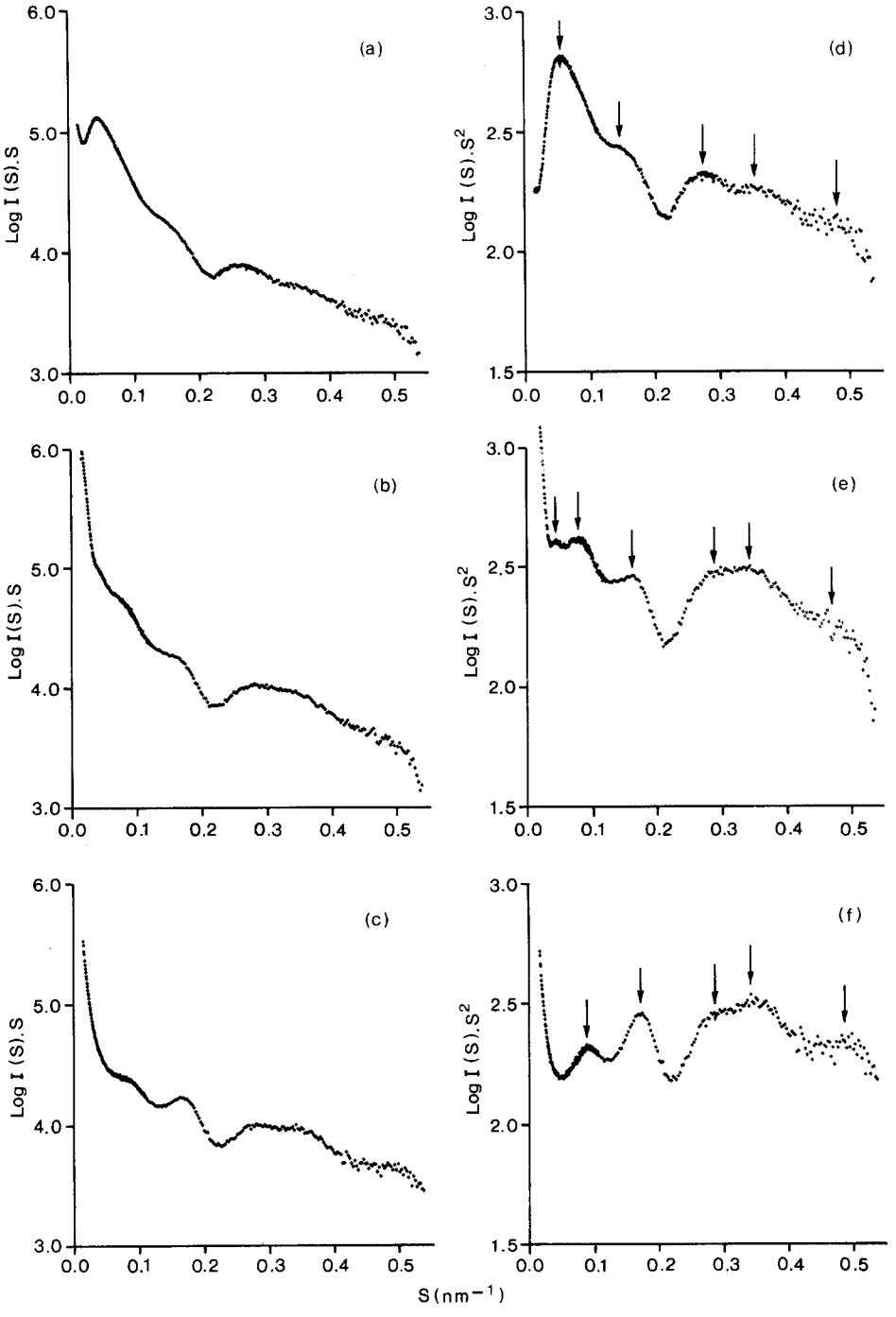

Fig. 2. X-ray scattering patterns of a 6.2 mg DNA/ml chromatin solution. **a** and **d** Typical pattern of chromatin-EDTA solutions. **b** and **e** Typical pattern obtained at high, but not maximal ionic strength, by addition of divalent cations (5 m*M* Mg^{++}). Similar patterns are obtained when the ionic strength is raised with NaCl (75–100 m*M*). **c** and **f** Patterns obtained upon further increase of the ionic strength (8 m*M* Mg^{++})

cation concentration relative to the chromatin concentration rather then the absolute concentration of cations. For instance, we found that at chromatin concentrations of 3.5 mg DNA/ml precipitation was noticeable with 3.5 m*M* $MgCl_2$ in the solution, while for 6.2 mg DNA/ml chromatin solutions the onset of precipitation did not occur for less than 8 m*M* $MgCl_2$. The same applied for aggregation as judged by the linearity of Porod plots.

As a result our data is not strictly comparable with light scattering studies (e.g. Ausio et al. 1984), where the chromatin concentrations used are of the order of hundred times lower and the fragments much shorter.

It is useful to consider two regions in the scattering pattern. Since the maximal dimensions of the core particle are $11 \times 11 \times 5.7\,nm^3$ the most prominent features in the very low angle region ($S < 0.09\,nm^{-1}$) must be associated solely with the distribution of the nucleosomes in the fibre, while features in the rest of the patterns may be associated with the internal structure of the nucleosomes. To a

first approximation the nucleosome structure does not change upon condensation, consequently, the changes in the scattering pattern must be associated with their redistribution when the fibre condenses.

Thus, the 0.05 nm^{-1} band can only arise from internal contrast in the superstructure of uncondensed chromatin. This is verified by its disappearance during condensation. The progressive increase of the maxima at 0.09 and 0.16–0.17 nm^{-1} must be due to the redistribution of the nucleosomes as condensation proceeds. These bands correspond to spacings of 11.0 and 5.8–6.2 nm respectively, these spacings are close to the dimensions of the nucleosomes and it is logical to interpret their origin as due to the packing of the nucleosomes when the fibre condenses. The fact that no other prominent bands develop argues strongly in favour of a closely packed structure leaving no prominent gaps.

A.2. Characterization of the X-ray scattering patterns from whole nuclei of chicken erythrocyte at high and at very low ionic strength. In the following experiments, the relationship between the isolated fibres in solution and in conditions more related to an "in vivo" situation was addressed. Figure 3 a and b show the scattering patterns from pellets of whole nuclei as $\log I(S) \times S$ and $\log I(S) \times S^2$ versus S respectively. The upper traces in both panels correspond to the patterns obtained at low ionic strength (nuclei-EDTA), while the lower traces were obtained in 100 mM NaCl (nuclei-NaCl).

The main features of the low ionic strength patterns are: A broad and strong band at 0.06 nm^{-1} which is absent in the high salt pattern, a prominent band at 0.156 nm^{-1}, a trough at 0.22 nm^{-1} and bands at 0.275 nm^{-1} and 0.36 nm^{-1}.

In high salt conditions one observes a weak band at 0.05 nm^{-1}, a band at 0.083 nm^{-1}, a prominent band at 0.15 nm^{-1}, a trough at 0.22 nm^{-1}, a prominent band at 0.275 nm^{-1} and a weak band near 0.36 nm^{-1}. At very low angles (ca. 0.023 nm^{-1}) both states exhibit the presence of a band not detected in the solution scattering patterns.

The pattern in physiological salt conditions (100 mM NaCl) is identical to those obtained in similar buffers by Langmore and Schutt (1980); Langmore and Paulson (1983).

Comparison between Figs. 2 and 3 reveals that in the region of S-values larger than 0.03 nm^{-1} one can identify common features with the patterns from chromatin fibres in solution whenever the measurements are carried out in near equivalent ionic conditions. The only bands observed in nuclei patterns which are clearly absent in the chromatin solution patterns are those at very low angles ($S \leq 0.023$ nm^{-1}). However, subtraction of the low

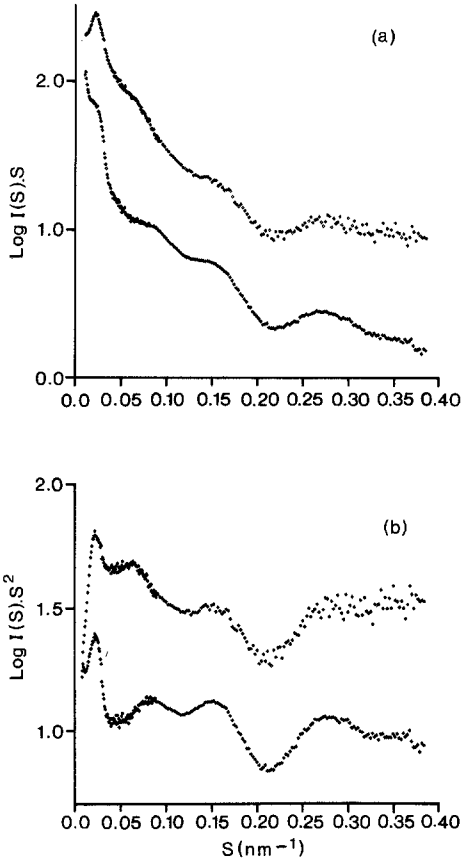

Fig. 3. X-ray scattering patterns from pellets of chicken erythrocyte nuclei

from the high ionic strength patterns from nuclei yields a nearly identical result (not shown) to the same operation performed on patterns from chromatin fibres in solution, showing that the changes induced by condensation of the fibre are very similar in both cases. The intensities in the bands at 0.023 nm^{-1} are nearly identical in high or in low salt conditions and the only difference is in the background on which the bands are superimposed. We refer here, of course, to the sample scattered background, rather than to the parasitic background which was removed in the data reduction procedures. Upon increasing the ionic strength, both in nuclei and in solutions, there is an increase in intensity for S values smaller than 0.03 nm^{-1}, a pronounced intensity reduction in a region centered around 0.05 nm^{-1}, the appearance of the band at 0.086 nm^{-1} and a strengthening of the pattern around the region of the broad band near 0.16 nm^{-1}.

The band at 0.023 nm^{-1} was not detected when the condensation of chromatin is induced by divalent cations ($MgCl_2$). An example of this result is shown in Fig. 4. The figure shows the very low angle part of the scattering patterns, notice that nuclei-EDTA

(Fig. 4a) and nuclei-NaCl (Fig. 4b) display a well defined band near $S = 0.023\ nm^{-1}$, while nuclei-Mg preparations (Fig. 4c) do not. Both nuclei-NaCl and nuclei-Mg preparations show the characteristic scattering band near $0.08\ nm^{-1}$ associated with the condensed state of the chromatin fibres (compare with Fig. 2). For nuclei-NaCl the centroid of the band is at slightly lower S-values (around $0.08\ nm^{-1}$ in this particular case) than for nuclei-Mg^{++} (around $0.08\ nm^{-1}$).

If the band at ca. $0.023\ nm^{-1}$ arises, as suggested by Langmore and Schutt (1980) and further verified by the results that follow, from interparticle interference effects due to the packing of chromatin fibres in the nuclei then these results would indicate that with divalent cations the chromatin fibres must be further apart.

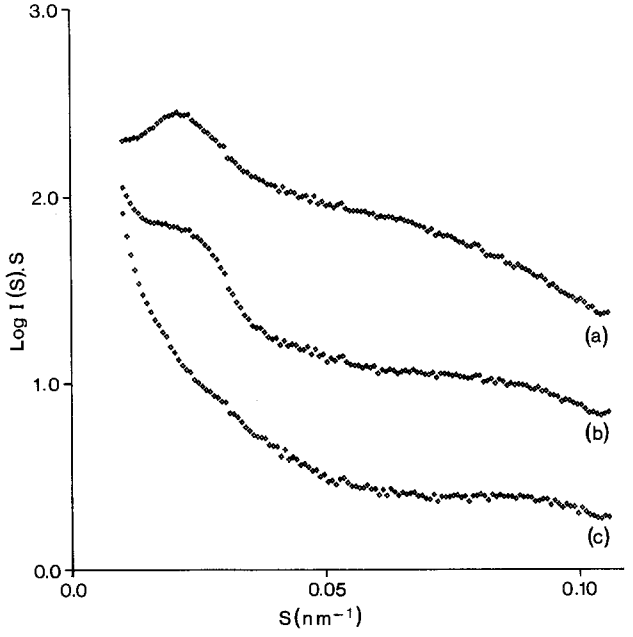

Fig. 4. Very low angle scattering patterns of chicken erythrocyte nuclei

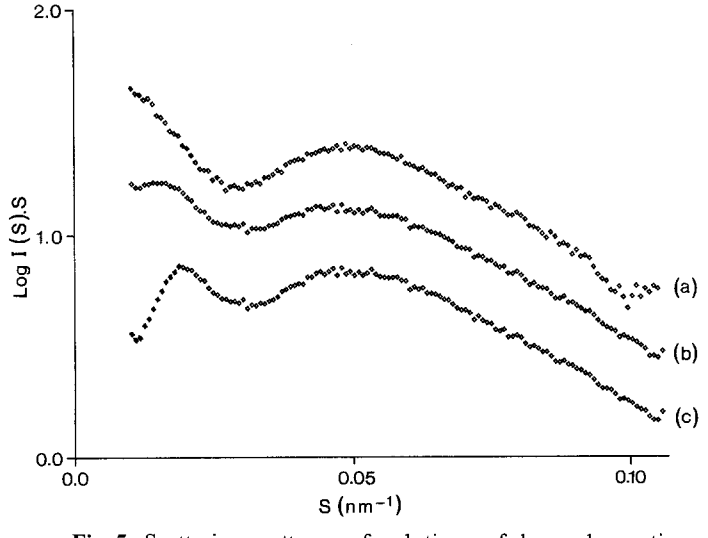

Fig. 5. Scattering patterns of solutions of long chromatin-EDTA fragments at different concentrations

A.3. Characterization of the X-ray scattering patterns from concentrated solutions of chromatin in very low and in high ionic strength buffers. The aim of these experiments was to increase the concentration of chromatin in the solution and bring the mean interfibre distance to a range comparable to the one in whole nuclei.

Figure 5 shows scattering patterns obtained from solutions of long chromatin fragments at different concentrations. The prominent band centered around $0.05\ nm^{-1}$ is present at 3 mg DNA/ml (Fig. 5a), 12 mg DNA/ml (Fig. 5b) and 16 mg DNA/ml (Fig. 5c). The relative intensity and position of this band are about the same in all three cases. However, with increasing concentration a band develops at very low angles, indicating the appearance of an interfibre interference effect. This interference band could not be made to move beyond $0.033\ nm^{-1}$ even for the most concentrated chromatin-EDTA preparations (see Perez-Grau et al. 1984 for more results of this kind).

The similarity of these patterns with that shown in Fig. 3a indicates a similar degree of packing of the chromatin-EDTA fibres in the nuclei.

These results indicate that, at increasing concentrations, the effects of a tighter packing of the chromatin fibres become detectable i.e. the very low angle band is due to an interfibre interference, whereas the $0.05\ nm^{-1}$ band is a feature characteristic of the native structure of the uncondensed chromatin fibre.

Even for the most concentrated gels, however, the interference band never moves to S-values higher than $0.033\ nm^{-1}$ (see Fig. 14 and Perez-Grau et al. 1984) indicating that to a first approximation the uncondensed nucleofilament has an outer diameter of around 30 nm.

The results of similar experiments performed by concentrating solutions of chromatin-NaCl and chromatin-$MgCl_2$, are illustrated in Fig. 6 (starting concentrations of 100 mM salt and 3 mM $MgCl_2$ respectively). The appearance of the very low angle band can be induced for chromatin-EDTA (Fig. 6a) and chromatin-NaCl (Fig. 6b) preparations. This was not possible with chromatin-Mg^{++} preparations (Fig. 6c), although the band at ca. $0.08\ nm^{-1}$, indicative of the condensed state of the chromatin fibre, can be detected and is in fact slightly better defined than in Fig. 6b. Even for extreme concentrations the interference band could not be observed (Fig. 6d). In this situation the $0.08\ nm^{-1}$ band is not

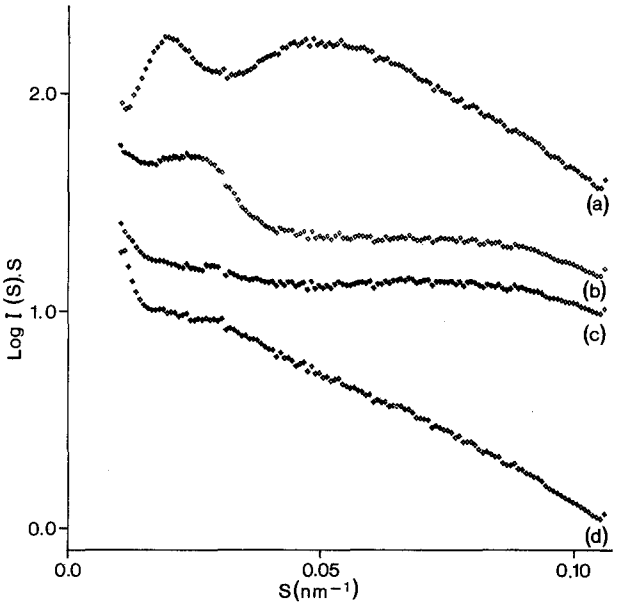

Fig. 6. Scattering patterns from concentrated solutions of chromatin-EDTA (*a*), chromatin-NaCl (*b*) and chromatin-Mg^{++} (*c* and *d*)

very prominent, possibly as a result of the disruption of the fibres due to the extended concentration procedure.

These observations correlate very well with those on whole nuclei, indicating a similar degree of packing of the chromatin fibres.

B. Characterization of the X-*ray scattering patterns of non-native chromatin:* X-*ray scattering patterns from solutions and gels of chromatin fibres depleted of the lysine rich histones and chromatin-fibres treated with ethidium bromide*

The aim of these experiments was to study the behaviour of the features in the scattering patterns from chromatin when the fibres are disrupted in a controlled manner.

B.1. X-*ray scattering from solutions and gels of chromatin depleted of the lysine rich histones* (H5). Figures 7a and b provide a comparison of the solution scattering patterns of chromatin-EDTA with those obtained under identical ionic conditions for chromatin depleted of the H1 (H5) histones whereas Fig. 7c and d give the equivalent comparison for gels of the same preparations. The PAGE analysis of the protein content of the preparations shown in Fig. 1 indicates that the removal of the H1 (H5) histones is complete.

Figure 7a and b provide a comparison between "native" chromatin-EDTA patterns and those obtained after removal of the H1 (H5) histones. The most prominent effects are the reduction of the slope of the scattered intensities at very low angles ($S < 0.03\ nm^{-1}$) and the shift of the $0.05\ nm^{-1}$ band to ca. $0.04\ nm^{-1}$ with an associated reduction of its relative intensity by about 2/3.

It can be deduced from the slope at very low angle that the radius of gyration of the cross-section has been reduced from ca. 10 nm for the native fibre to around 5.7 nm after depletion of the H1 (H5) histones. Figure 7c and d provide an equivalent comparison for gels. Notice that in the case of chromatin depleted of H1 (H5) the interference band at low angle can be made to shift to around 0.06 nm (Fig. 7d), perhaps superimposing on the characteristic 0.05 nm band of "native" chromatin-EDTA preparations.

These results provide evidence that the H1 (H5) histones are responsible for keeping the low ionic strength chromatin fibres in a kind of extended helical structure and that upon their removal the fibre extends, simultaneously reducing its mean diameter and increasing its pitch. The appearance of the chromatin fibre depleted of H1 (H5) histones probably resembles the "zig-zag" structure often observed in electron micrographs.

B.2. X-ray scattering from solutions of chromatin treated with ethidium bromide. It is well known that DNA has a considerable affinity for basic dyes like ethidium bromide, a planar molecule which intercalates between successive base pairs, causing a local unwinding and lengthening of the DNA double helix (Lerman 1961; Fuller and Waring 1964). The DNA unwinding angle per ethidium molecule bound is about 26° (Wang 1974). Ethidium binding to DNA in low salt does not displace the histones (Benyajati and Worcel 1976). Hence, progressive binding of Ethidium Bromide should unwind and

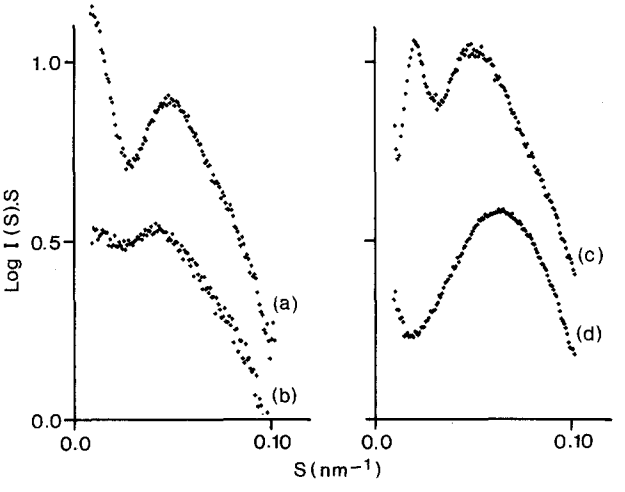

Fig. 7. Changes induced in the scattering patterns of solutions (*a* and *b*) and gels (*c* and *d*) of chromatin-EDTA preparations upon removal of the lysine rich histones

lengthen the DNA, starting with the linker and progressively disrupting the whole fibre.

Figure 8 illustrates the effects of increasing concentrations of ethidium bromide in the chromatin-EDTA (3.5 mg DNA/ml) X-ray scattering patterns: (0 m*M*: Fig. 8 a; 0.1 m*M*: Fig. 8 b; 0.2 m*M*: Fig. 8 c; 0.5 m*M*: Fig. 8 d; 0.7 m*M*: Fig. 8 e and 1.0 m*M*: Fig. 8 f).

The 0.05 nm^{-1} band progressively moves towards lower values of the scattering vector, while its prominence simultaneously decreases. The slope at low angles reaches a minimum at about 0.7 m*M* ethidium bromide (Fig. 8 d). At 0.05 m*M* ethidium bromide the 0.05 nm^{-1} band has shifted to about 0.035 nm^{-1} and its onset is at 0.025 nm^{-1}. At 0.7 m*M* ethidium bromide this band is still visible above the background although with a much more reduced intensity. These trends are comparable, although more pronounced, to those observed upon removal of the H1 (H5) histone and they indicate that an increase of the helical pitch is concomitant with the reduction of the mean diameter (i.e. shift of the 0.05 nm^{-1} band to lower angles and reduction of the slope in the central scatter) as the fibre is progressively extended.

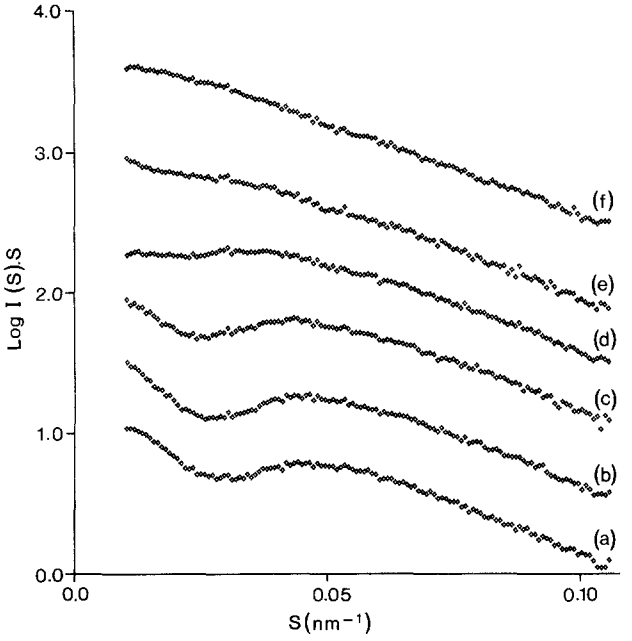

Fig. 8. Changes in the very low angle scattering patterns from chromatin-EDTA fibres induced by increasing amounts of bound ethidium bromide

C. Development of the small angle scattering patterns of "native" chromatin fibres as a function of ionic strength

Figure 9 provides an example of the behaviour of the low angle region in the scattering patterns of chromatin solutions at various concentrations of $MgCl_2$. The results belong to the same series as the patterns displayed in Fig. 2 (6.2 mg DNA/ml concentration of "native" chromatin fibres). When other concentrations of chromatin were tried, it was found that the concentration of cations had to adjusted to the correct ratio in order to obtain identical patterns.

The patterns correspond to: Chromatin-EDTA (Fig. 9 a) and chromatin-EDTA with increasing amounts of $MgCl_2$ (1, 1.5, 2, 2.5, 3, 4, 5, 6, 7 and 8 m*M* $MgCl_2$ shown in Fig. 9 b to k respectively).

Upon increase of the ionic strength the 0.05 nm^{-1} band shifts to higher angles and simultaneously decreases in intensity. The central scatter ($S \leq 0.03$ nm), rises nearly continuously with increasing amounts of $MgCl_2$. There is the fleeting appearance of a weak band at 0.045 nm^{-1} at around 5 m*M* Mg^{++} concentration (Fig. 9 h), which disappears at even higher ionic strength. The 0.09 nm^{-1} band is only clearly established at the maximum cation concentration.

These observations suggest that the helical pitch responsible for the band at 0.05 nm^{-1} disappears before the chromatin fibre is fully condensed. At

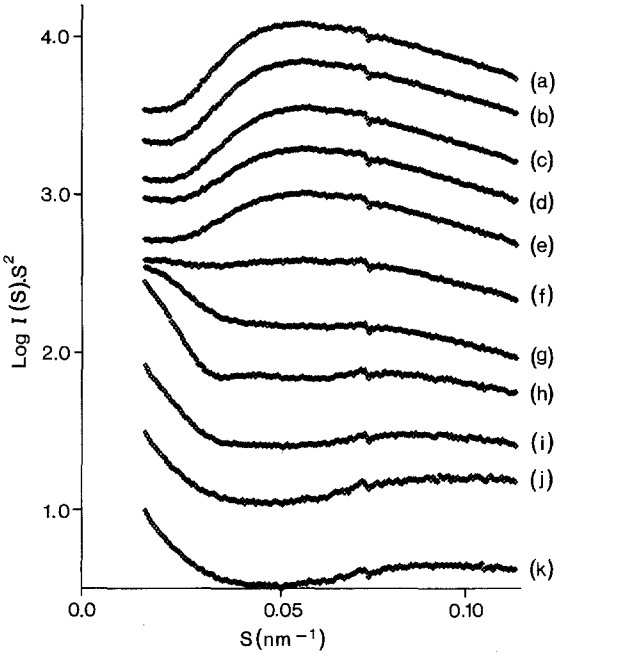

Fig. 9. Development of the solution scattering patterns of "native" chromatin-EDTA fragments upon increasing the ionic strength by means of divalent cations

relatively low ionic strength this band begins to shift to higher angles and there is an intermediate state of condensation (e.g. Fig. 9 f) in which this band is centered around 0.065 nm^{-1}. Simultaneously the radii of gyration of the cross-section and the mass per unit length have increased but not yet reached

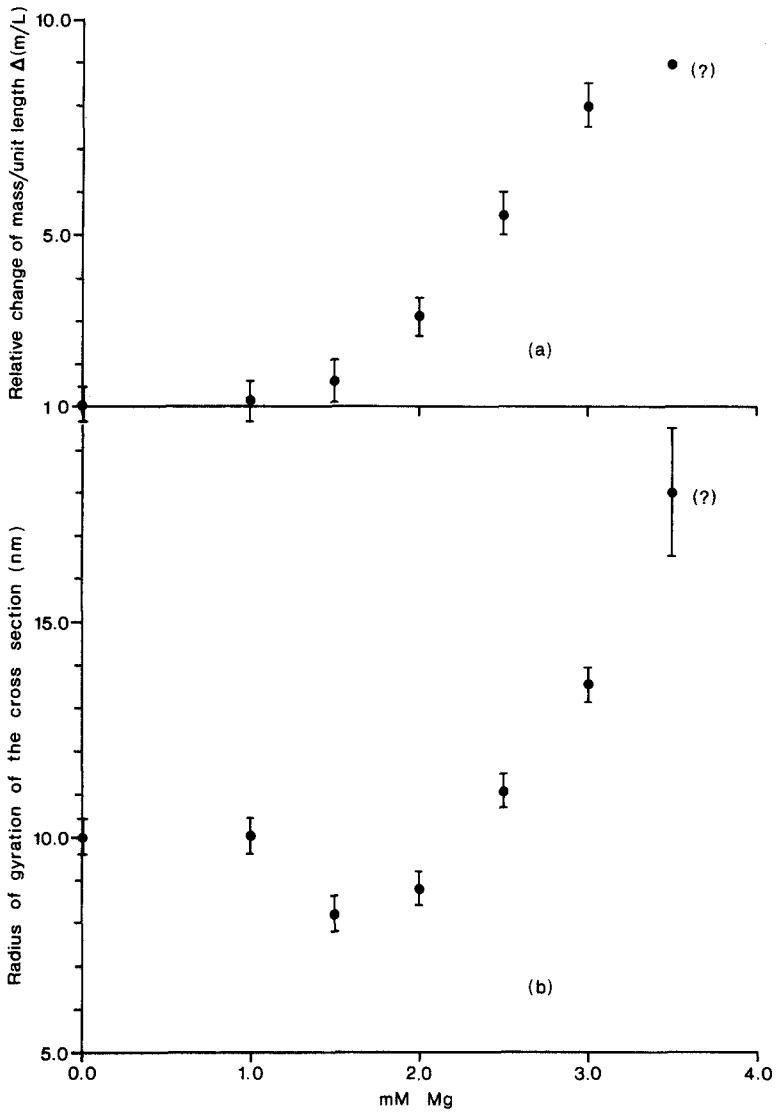

Fig. 10. Relative changes in the mass per unit length (**a**) and changes in the radii of gyration of the cross-section for chromatin-EDTA fibres (3.5 mg DNA/ml) with increasing concentrations of Mg cations

their maximum value as discussed in Sect. D and illustrated in Figs. 10 and 11.

The observations are consistent with a model in which the pitch of the uncondensed structure progressively diminishes as the fibre is on its way to maximal compaction.

When condensation is induced by addition of NaCl the scattering patterns display qualitatively similar trends but as discussed in the following section there are quantitative differences.

D. Model independent structural parameters from X-ray solution scattering of chromatin: Radii of gyration of the cross section and relative changes of mass per unit length

D.1. Condensation of chromatin fibres by means of divalent ($MgCl_2$) *and monovalent* (NaCl) *cations.* The different effects induced by addition of $MgCl_2$ and NaCl are illustrated in Figs. 10 and 11. The data shown were derived from measurements in the very low angle part of the scattering patterns from "native" chromatin solutions at 3.5 mg DNA/ml concentration.

Figures 10a and 11a correspond to the measured changes in the relative mass per unit length on addition of $MgCl_2$ and NaCl respectively, while Figs. 10b and 11b display the accompanying changes in the radii of gyration of the cross-section. For both types of cations the radii of gyration of the cross-section markedly drop at low ionic strengths. The values are considerably smaller at about 30 m*M* NaCl or 1.5 m*M* $MgCl_2$ than in the uncondensed state. At higher ionic strengths the radii of gyration increase and exceed the starting value for chromatin-EDTA (Figs. 10b and 11b respectively). The main difference is that while for $MgCl_2$ the mass per unit length and the radius of gyration increase until precipitation takes place, for NaCl induced condensation they show a saturation effect.

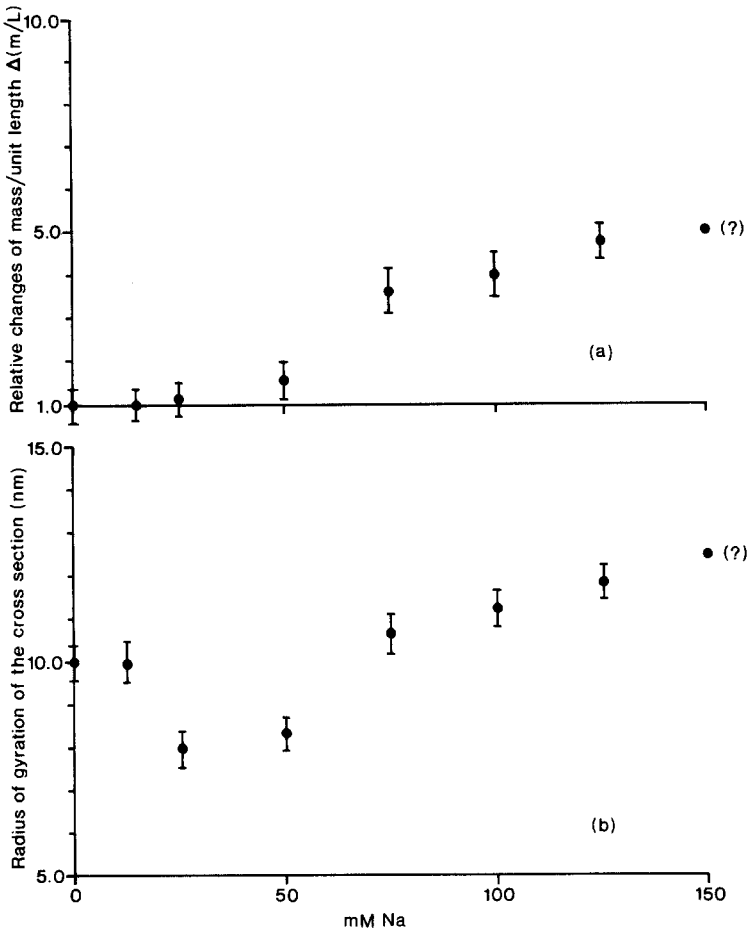

Fig. 11. Relative changes in the mass per unit length (**a**) and changes in the radii of gyration of the cross-section for chromatin-EDTA fibres (3.5 mg DNA/ml) with increasing concentrations of NaCl

These results are consistent with the sedimentation measurements of Butler and Thomas (1980); Thomas and Butler (1980) which indicated a jump in the measured sedimentation coefficient at about 40–45 m*M* NaCl. The interpretation put forward by these authors was that the uncondensed chromatin fibre undergoes a stabilization, leading to a faster sedimentation rate.

Our observations also indicate that the radius of gyration of the cross-section significantly decreases at around this ionic strength, while the mass per unit length has begun to increase. These data suggest that full compaction of the fibre is only reached at ionic strengths just before precipitation, which in this particular concentration of chromatin was noticeable at ca. 3.5 m*M* Mg^{++} or 150 m*M* salt respectively. The points in Figs. 10 and 11 identified with a question mark are suspect because of this reason.

The ratio between the maximum mass per unit length obtained before noticeable precipitation took place and the starting value, was around 8 and 4 times for condensation induced by divalent (Mg^{++}) and monovalent (Na^{+}) cations respectively. The different effects of $MgCl_2$ or NaCl in the induced condensation is also reflected in the values reached by the radii of gyration of the cross-section, which were considerably higher for divalent (Mg^{++}) than for monovalent (Na^{+}) cations. The maximum values reliably measured were 13.5 and 11.9 nm for Mg^{++} and Na^{+} cations, respectively. These values correspond to equivalent solid cylinders with outer diameters of about 38.0 and 33.0 nm respectively. They should be compared with the equivalent diameter of chromatin-EDTA (28 nm).

Thus, for this concentration of chromatin, the final diameter of the condensed chromatin fibre is larger and the fibre more compacted at 3 m*M* $MgCl_2$ than at, say, 100 m*M* NaCl. In the latter case the diameter is closer to that of the uncondensed chromatin-EDTA state, although its mass per unit length is larger. These results corroborate the interpretation of the observations on whole nuclei and gels, according to which the larger mean diameter of the fibres in $MgCl_2$ should result in an interference peak occurring for S-values outside the range of observation.

Thus, $MgCl_2$ induces a higher degree of compaction of the chromatin fibre than NaCl. This is also supported by the fact that the 0.09 nm^{-1} band ap-

pears to be better defined in $MgCl_2$ than in NaCl. Electron micrographs of chromatin in $MgCl_2$ also indicate that these fibres appear as more compact objects than in NaCl (Azorin et al. 1982).

Jermanowski and Staron (1981) have argued that closer packing of the nucleosomes in mitosis must be connected with a loss of bound water as new hydrophobic interactions in chromatin are generated by neutralization of the excess negative charges on the DNA. In this respect it is perhaps significant that the measured maximum state of condensation takes place at concentrations of divalent cations close or identical to those needed to induce precipitation. Also highly raised levels of divalent cations have been detected in condensed chromosomes in a variety of dinoflagellates (Sigee 1982 and references therein). The various observations argue in favour of the need of divalent cations for complete condensation of the chromatin fibres as well as for a specifity in their action.

Measurements of the radius of gyration of the cross-section of chromatin fibres depleted of the H1 (H5) histones yield a value of 5.7 nm, also indicating that the fibres have lost their three-dimensional organization.

D.2. Effects of ethidium bromide on the radii of gyration of the cross-section and on the mass per unit length of chromatin fibres. Figure 12 a and b show the results from measurements of the radii of gyration of the cross-section and changes of mass per unit length on chromatin-EDTA fibres treated with ethidium bromide. The concentration of chromatin was 3.5 mg DNA/ml.

For increasing amounts of bound ethidium bromide up to 0.5 m*M* concentrations, one finds that both the radii of gyration of the cross-section and the relative mass per unit length decrease, respectively reaching a minimum value of 3.6 nm and 0.38–0.4 at 0.5 m*M* ethidium bromide.

At higher concentrations of ethidium bromide the trend apparently reverses but the remnants of the 0.05 nm^{-1} band may be superimposed on the small angle region (Fig. 8) thus precluding a meaningful determination of the radius of gyration of the cross-section and of the relative changes of mass per unit length.

These results are consistent with a model in which in helical uncondensed chromatin fibre unwinds, lengthens and acquires a "string of beads" configuration. Both, the decrease of mass per unit length and the radii of gyration of the cross-section are consistent with this behaviour. The reversal of the behaviour observed above 0.5 m*M* ethidium bromide concentration could also mean that the chromatin fibre may wind up with the opposite hand.

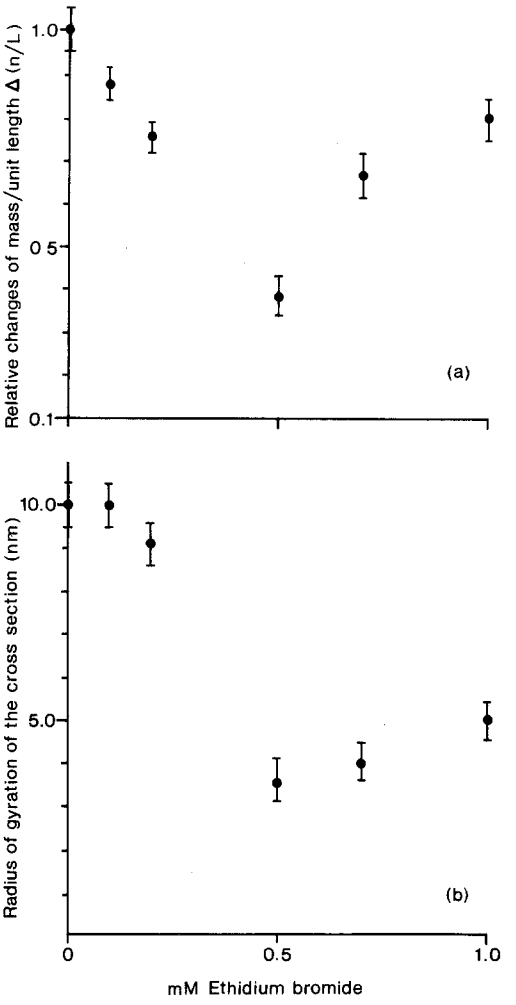

Fig. 12. Changes in the relative values of the mass per unit length (**a**) and of the radii of gyration of the cross-section (**b**) for chromatin-EDTA (3.5 mg DNA/ml) with increasing concentrations of ethidium bromide

Together with the results shown in Fig. 10, these data indicate that fully condensed chromatin must have a mass per unit length in excess of twenty times than that of its most extended configuration.

E. Condensation kinetics of chromatin in solution and in concentrated gels

Time-resolved X-ray scattering measurements on chromatin solutions indicate that the condensation of native chromatin fibres is a very fast process.

X-ray stopped flow experiments on chromatin solutions showed that chromatin submitted to an ionic jump condenses with a time constant of less than 50 ms (data not shown).

Condensation kinetics of chromatin gels were also studied. Since the use of the X-ray stopped flow device was precluded by the high viscosity of the preparation the buffer was diffused into the gels by

depositing a drop, at the desired ionic strength, on top of the sample.

Even in very compacted gels the condensation process is fast and independent of the use of monovalent or divalent cations. Condensation of chromatin fibres can also be induced by diffusing excess EDTA instead of cations and, in the resolution range of these measurements, the condensed state was indistinguishable.

Results of a condensation achieved by diffusing a buffer containing excess EDTA (500 mM) into a chromatin gel are illustrated by Figs. 13 and 14.

Figure 13a shows a correlation plot of the integrated scattered intensities for S-values smaller than 0.025 nm^{-1} versus the scattered intensities at about 0.05 nm^{-1}. In this type of plot any departure from a straight line indicates the onset of a different structural modification of the object in solution (see

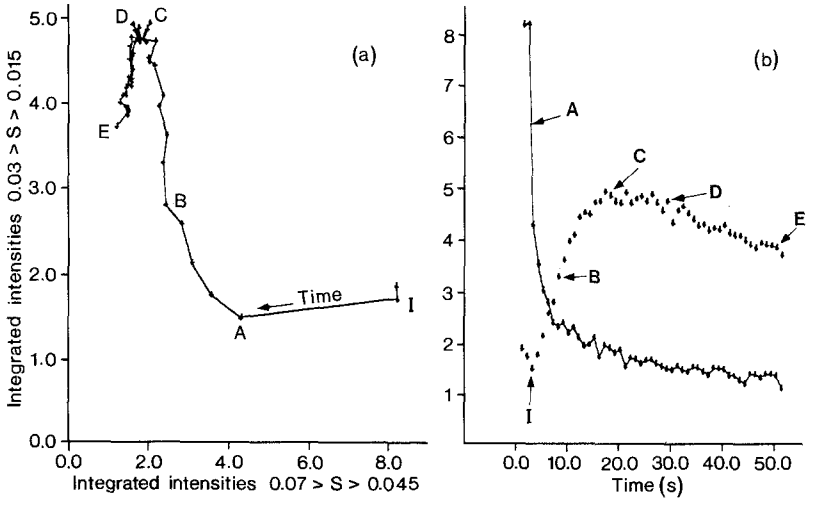

Fig. 13a and b. Correlation plot of the integrated intensities scattered for values of $0.015 \leq S \leq 0.03$ nm^{-1} (vertical axis) and at $0.045 \leq S \leq 0.07$ nm^{-1} (horizontal axis) and their corresponding time dependence (**a** and **b** respectively) for chromatin-EDTA gels undergoing condensation. The arrow in (**a**) indicates the time direction

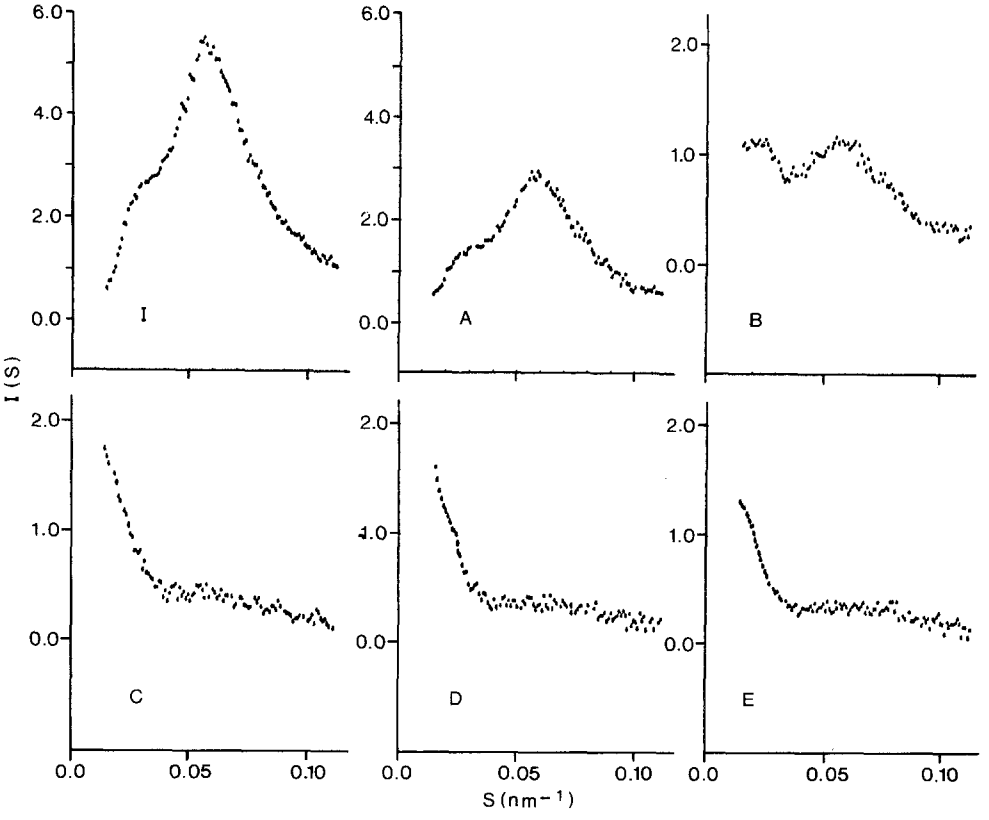

Fig. 14 I, A–E. Condensation of chromatin-EDTA gels. The patterns shown have been selected to coincide in time with the intermediate states detected by the correlation analysis and the time courses shown in Fig. 13

Bordas et al. 1983). Starting from the initial state (I) various departures from linearity (A, B, C, D, E) point to a series of intermediate states.

Figure 13 b shows the development of these scattered intensities as a function of time. The very low angle region is characterized by a small decrease in intensity (I to A) followed by a fast rise (A–B–C) which precedes a second slower decrease in intensity (C–D–E). The time course in the second region shows a continuous drop, very pronounced between A and B and much gentler between B and E. The data shown in Fig. 13 allow us to postulate the existence of various different processes occurring at times A, B, C, D, and E.

The individual scattering patterns are shown in Fig. 14. From their analysis and comparison, one can propose the following sequence of events: When the buffer is dropped one first observes a dilution effect (I to A). The starting scattering pattern shows the familiar band at about 0.05 nm^{-1} (which is in itself an indication of the integrity of the fibres) and an interference band at 0.03 nm^{-1}. The position of this band is in itself an indication of the high degree of compaction of the chromatin fibres in the gel (33 nm mean distance between the fibres). The dilution effect between times I and A is reflected by a general decrease in the scattered intensity in the otherwise congruent scattering patterns. Between times A and C the interference band moves behind the beam stop because as the fibres condense their volume becomes smaller and the interfibre distance can become larger. At the intermediate time B one can still observe the remnants of the interference band now centered at about 0.02 nm^{-1} (i.e. 50 nm mean distance between fibres). The change in slope in the correlation plot at B occurs because after this point one is no longer sensitive to the influence of the interparticle interference on the scattering pattern. Notice that at time B the scattering pattern is comparable to that obtained in whole nuclei. At C the condensation process is nearly complete resulting in the appearance of the characteristic scattering pattern. From C to E the effects might indicate a redistribution in the condensation state of the fibres.

These results clearly show that even in very concentrated gels the condensation process is also fast (half time of ca. 5 s). In fact, most of the lag time in the condensation, if not all, is accounted for by the dilution and diffusion of the condensing agent.

4. Discussion

The value of 10.0 nm for the radius of gyration of uncondensed chromatin (Sect. D), the presence of the interference band at 0.023 nm^{-1} in nuclei at low ionic strength (Sect. A.2) and the behaviour of this interference band, which even at the highest concentration of chromatin cannot be forced to appear at spacings of less than 30.0 nm (Sect. A.3), provide three independent sources of evidence indicating that uncondensed chromatin has a much larger diameter than could be expected from an extended "string of beads" model. The maximum value for the radius of gyration of the cross-section that can be expected from an extended nucleofilament model, given the dimensions of the nucleosomes, is around 3.6 nm. This value is much smaller than that provided by these three different types of experiments. These findings suggests that the uncondensed chromatin fibre, whether in solution or in the more native nuclei environment, already has a higher level of folding which confers to it a three dimensional organization.

Moreover, this three dimensional organization has to account for the persistent presence of the 0.05 nm^{-1} band in solutions (Sect. A.1), nuclei (Sect. A.2) and gels (Sect. A.3 and E).

From these observations alone, a picture emerges in which uncondensed chromatin already has a preformed helical superstructure in which the 0.05 nm^{-1} band is probably due to the contrast arising from the helical pitch. This band is highly assymmetric in shape, i.e. it has a sharp leading edge with its onset at ca. 0.03 nm^{-1}, goes to a maximum at 0.05 nm^{-1} and it decays more smoothly at higher angles (see Fig. 2 or, shown more clearly, Fig. 9 a). This is the shape expected from a near meridional maximum in a disoriented fibre diffraction diagram. In this situation, the pitch of the helix coincides with the onset of the band (at ca. 0.03 nm^{-1}) rather than with its maximum, which corresponds to the distance between neighbouring nucleosomes in the superstructure.

Further support for this model is provided by the results obtained on the disrupted fibres. The results described in Sect. B.1 show that this structural scaffolding is maintained by the H1 (H5) histones. The observation that upon removal of these histones the 0.05 nm^{-1} band is displaced to lower values of S (i.e. the pitch becomes larges) and that the radius of gyration of the cross-section goes down to 5.4 nm (Sect. D) and that the interference maximum in the gels can shift to higher values of S (Sect. B.1), are all supportive of the existence of this superstructure in uncondensed chromatin. These results are in very good agreement with the electron microscopy of Thoma and Koller (1977) who observed a much more extended fibre after removal of the H1 (H5) histones. Although the outer diameter of "native" uncondensed chromatin is similar to that

found in the condensed state induced by salt, its structure is more extended and the nucleosomes are more exposed to the solvent. Upon removal of H1 (H5) histones the fibre would have an appearance closer to the string-of-beads model or perhaps more like the "zig-zag" structure seen in electron microscopy (Thoma and Koller 1977). In fact, the radius of gyration of the cross-section for chromatin fibres depleted of the H1 (H5) histones is more compatible with the latter possibility than with the former. The H1 (H5) histones confer to this string-of-beads the structural organization of a "helical string of beads" and the 0.05 nm^{-1} band, characteristic of uncondensed "native" chromatin arises mainly from the helical pitch typical of this state. This picture of uncondensed chromatin is further supported by the results described in Sect. B.2. When ethidium bromide is bound to the fibres and the linker DNA progressively unwinds extending the open superhelix of the uncondensed chromatin, its pitch giving rise to the 0.05 nm^{-1} increases in a manner similar to the effect of H1 (H5) removal. In the latter case, however, the results indicate that the fibre does not become fully extended, while with ethidium bromide the lengthening process leads to a situation that one could describe as a "straight string of beads" as opposed to a "zig-zag string of beads".

This interpretation is reinforced by the results shown in Sect. D.2, which show that upon binding ethidium bromide, the decrease of the mass per unit length and of the radius of gyration of the cross-section is consistent with a progressive unwinding and lengthening of the superstructure in the uncondensed fibre. The results show that the mass per unit length at 0.5 m*M* ethidium bromide is about 2.5–2.6 smaller than in "native" uncondensed chromatin, while the radius of gyration of the cross-section has a value of 3.6 nm, which closely corresponds to that expected from a fully extended nucleofilament. These results suggest that the "native" uncondensed chromatin fibre has at least 2.5–2.6 nucleosomes per turn of a helical structure with a pitch of around 33.0 nm (i.e. the onset of the 0.05 nm^{-1} band) and an outer diameter of around 30.0 nm.

This picture of the uncondensed state of chromatin is quite different from that previously derived from electron microscopy, X-ray and neutron scattering experiments (Olins and Olins 1974; Sperling and Tardieu 1976; Suau et al. 1979), but agrees quite well with some suggestions recently put forward (Thoma and Koller 1981; Campbell et al. 1978; Shaw and Schmitz 1979; Marion et al. 1981).

Upon increase in the ionic strength this already preformed helical string of beads undergoes a compaction comparable to the folding of an accordion, where the outer diameter does not change significantly when compared to the change of length. The results shown in Sect. C are supportive of this mechanism, they illustrate how upon condensation the 0.05 nm^{-1} band progressively moves to higher values of S while the fibres settle into a new helical configuration. This is the behaviour expected from this kind of mechanism. The observed reduction in intensity is also expected, because as the nucleosomes make contact the electron density contrast is bound to decrease.

The transition from uncondensed to condensed chromatin goes through a series of intermediate states and divalent cations appear to be much more effective condensing agents than salt (Sect. D). The data also indicates that maximal condensation coincides with precipitation (i.e. fully condensed chromatin is not soluble). This is demonstrated not only by the results described in section D but also by the fact that the diffraction bands characteristic of the condensed state (i.e. the 0.09, 0.16–0.17 nm^{-1} bands) are much better defined in conditions close to or equal to those needed to induce precipitation (see Sect. A.1 and Fig. 2).

Finally this mechanism of condensation is supported by the measurements described in section E, which prove that even in very concentrated gels condensation is a fast process. With an extended structure like the "string of beads" model, it would be very difficult to envisage that such a process could happen without tangling whereas with the proposed preformed structure the possibilities of tangling are minimized. Conceivably, the situation in the cell nucleus might not be too different from that in concentrated gels. The process of condensation in the chromosomes could be controlled by rapid changes of the helical pitch of the superhelical structure. Furthermore, the accordion-like structure would, of course, not need to stretch along its full length: Stretching may occur in selected areas if, for instance, a site recognizing enzyme induces local unfolding of the chromatin.

The results in Sect. E also indicate that independently of the condensing agent any sufficiently large change in the balance of charges might achieve at least partial condensation as suggested by the fact that the effect of an excess EDTA is comparable to that of salt but that it is possible that only certain cations might be capable of inducing complete condensation. The absence of an interference maximum in Mg-nuclei (Sect. A.2), Mg-chromatin gels (Sect. A.3) and the higher values of the radius of gyration of the cross-section and increase of mass per unit length for Mg induced condensation (Sect. D.1) indicate that Mg is capable of inducing a higher level of condensation than salt.

On the basis of the measurements of the changes of mass per unit length one can conclude that for the structure to fold in an accordion like fashion, the helical pitch of the superstructure has to decrease from around 30.0 nm (onset of the 0.05 nm^{-1} band) down to 8 or 9 times less, i.e. in the region of 3.0 to 4.0 nm. Simultaneously the nucleosomes must tightly pack leaving no prominent electron density grooves in the fibres as judged by the development of only the 0.09 and 0.16 nm^{-1} bands which are due to the close packing of the nucleosomes.

Acknowledgements. We thank the staff of the European Molecular Biology Laboratory Outstation at Hamburg (DESY) for their support during the course of this work.

This work was supported by a grant from the Deutscher Akademischer Austauschdienst (DAAD) to M.C. Vega.

L. Perez-Grau Was the recipient of an EMBL post-doctoral fellowship.

References

Ausio J, Borochov N, Seger D, Eisenberg H (1984) Interaction of chromatin with NaCl and $MgCl_2$. J Mol Biol 177: 373–398

Azorin F, Perez-Grau L, Subirana JA (1982) Supranucleosomal organization of chromatin. Chromosoma 85:251–260

Bates DL, Butler PJG, Pearson EC, Thomas JO (1981) Stability of the higher-order structures of chicken-erythrocyte chromatin in solution. Eur J Biochem 119:469–476

Benyajati C, Worcel A (1976) Isolation, characterization and structure of the folded interphase genome of *Drosophilia melanogaster*. Cell 9:393–407

Bolund LA, Johns EW (1973) The selective extraction of histone fractions from deoxyribonucleoprotein. Eur J Biochem 35:546–553

Bordas J, Koch MHJ, Clout PN, Dorrington E, Boulin C, Gabriel A (1980) A synchrotron radiation camera and data acquisition system for time resolved X-ray scattering studies. J Phys E 13:938–944

Bordas J, Mandelkow EM, Mandelkow E (1983) Stages of tubulin assembly and disassembly – studied by time resolved synchrotron X-ray scattering. J Mol Biol 164: 89–136

Borochov N, Ausio J, Eisenberg H (1984) Interaction and conformational changes of chromatin with divalent cations. Nucleic Acids Res 12:3089–3096

Boulin C, Dainton D, Dorrington E, Elsner G, Gabriel A, Bordas J, Koch MHJ (1982) Systems for time resolved X-ray measurements using one-dimensional and two-dimensional detectors. Nucl Instrum Methods 201:209–220

Butler PJG, Thomas JO (1980) Changes in chromatin folding in solution. J Mol Biol 140:505–529

Campbell AM, Cotter RI, Pardon JF (1978) Light scattering measurements supporting helical structures for chromatin in solution. Nucleic Acids Res 5:1571–1580

Damaschun H, Damaschun G, Pospelov VA, Vorob'ev VI (1980) X-ray small angle scattering study of mononucleosomes and the close packing of nucleosomes in polynucleosomes. Mol Biol Rep 6:185–191

Fedorov BA, Aleshin VG (1966) Theory of small angle X-ray scattering by long rigid macromolecules in solution. Vysokomol Soedin 8:1506–1513

Finch JT, Klug A (1976) Solenoidal model for superstructure in chromatin. Proc Natl Acad Sci USA 73:1879–1901

Fuller W, Waring MJ (1964) A molecular model for the interaction of ethidium bromide with deoxyribonucleic acid. Ber Bunsenges Phys Chem 68:805–811

Fulmer AW, Bloomfield VA (1982) Higher order folding of two different classes of chromatin isolated from chicken erythrocyte nuclei. A light scattering study. Biochemistry 21:985–992

Garret RA (1971) Low angle X-ray diffraction from dilute nucleohistone gels. Biochim Biophys Acta 246:553–560

Guinier A, Fournet G (1955) Small angle scattering of X-rays. John Wiley, New York

Hendrix J, Koch MHJ, Bordas J (1979) A double focussing X-ray camera for use with synchrotron radiation. J Appl Crystallogr 1979:467–472

Hjelm RP, Kneale GG, Suau P, Baldwin JP, Bradbury EM, Ibel K (1977) Small angle neutron scattering studies of chromatin subunits in solution. Cell 10:139–151

Jermanowski A, Staron K (1981) Can phosphorylation of histone H1 be responsible for chromatin condensation in mitosis? J Theor Biol 89:191–194

Koch MHJ, Bendall P (1981) INSCOM: An interactive data evaluation program for multichannel analysis-type data. Proceedings of the Digital Equipment Users Society, 13–16, DECUS, U.K.

Koch MHJ, Bordas J (1983) X-ray diffraction and scattering on disordered systems using synchrotron radiation. Nucl Instrum Methods 208:435–438

Kratky O, Porod G (1953) Die Physik der Hochpolymere, Vol II. Springer-Verlag, Berlin Göttingen Heidelberg

Laemmli UK (1970) Cleavage of structural proteins during the assembly of the head of bacteriophage T4. Nature 227:680–685

Langmore JP, Paulson JR (1983) Low angle X-ray diffraction studies of chromatin structure in vivo and in isolated nucleii of metaphase chromosomes. J Cell Biol 96: 1120–1131

Langmore JP, Schutt C (1980) The higher order structure of chicken erythrocyte chromosomes in vivo. Nature 288: 620–622

Lerman LS (1961) Structural considerations in the interaction of DNA and acidines. J Mol Biol 3:18–30

Loening VE (1967) The fractionation of high molecular weight ribonucleic acid by polyacrylamide gel electrophoresis. Biochem J 102:251–263

Luzatti V (1960) Interpretation des mesure absolues de diffusion centrale des rayons Y en collimation ponctuelle ou lineaire: Solutions de particules globulaires et de batonnets. Acta Crystallogr 13:939–945

Luzatti V, Nicolaieff A (1959) The structure of nucleohistones and nucleoproteins. J Mol Biol 1:127–133

Marion C (1984) The structural organization of oligonucleosomes. J Biomol Struct Dynamics 2:303–316

Marion C, Bezot P, Hesse-Bezot C, Roux B, Bernengo JC (1981) Conformation of chromatin oligomers. A new argument for a change with the hexanucleosome. Eur J Biochem 120:169–176

Noll M, Thomas JO, Kornberg RD (1975) Preparation of native chromatin and damage caused by shearing. Science 187:1203–1206

Notbohm H, Harbers E (1981) Small angle X-ray scattering of intact and lysing all nuclei. Int J Biol Macromol 3:311–314

Olins AL, Olins DA (1974) Spheroid chromatin units (U-bodies). Science 183:330–332

Olins AL, Carlson RD, Wright EB, Olins DE (1976) Chromatin bodies: Isolation, to subfractionation and physical characterization. Nucleic Acids Res 3:3271–3291

Paulson JR, Langmore JP (1983) Low angle X-ray diffraction studies of hela metaphase chromosomes: Effects of histone

phosphorylation and chromosome isolation procedure. J Cell Biol 96:1132–1137
Perez-Grau L, Bordas J, Koch MHJ (1984) Chromatin superstructure: Synchrotron radiation X-ray scattering study on solutions and gels. Nucleic Acid Res 6:2987–2995
Renner W, Mandelkow EM, Mandelkow E, Bordas J (1983) Self-assembly of microtubule protein studied by time-resolved X-ray scattering using temperature jump and stopped flow. Nucl Instrum Methods 208:535–540
Richards B, Pardon J, Lilley D, Cotter R, Wooley J, Worcester DL (1977) The sub-structure of nucleosomes. Cell Biol Int Rep 1:107–116
Shaw BR, Schmitz (1979) Conformation of polynucleosomes in low ionic strength solution. In: Nicolini CA (ed) Chromatin structure and function (Part B), Plenum Press, New York, pp 427–439
Sigee DC (1982) Localised uptake of nickel into dinoflagellate chromosomes: An autoradiographic study. Protoplasma 110:112–120
Sothern E (1980) Gel dectrophoresis of restriction fragments. Methods Enzymol 68:152–163
Sperling L, Klug A (1977) X-ray studies on "native" chromatin. J Mol Biol 112:253–263
Sperling L, Tardieu A (1976) The mass per unit length of chromatin by low-angle X-ray scattering. FEBS Lett 1:89–91
Suau P, Bradbury EM, Baldwin JP (1979) Higher-order structures of chromatin in solution. Eur J Biochem 97:593–602
Thoma F, Koller T (1977) Influence of histone H1 on chromatin structure. Cell 12:101–107
Thoma F, Koller T (1981) Unravelled nucleosomes, nucleosome heads and higher order structures of chromatin: Influence of non-histone components and histone H1. J Mol Biol 149:709–733
Thoma F, Koller T, Klug A (1979) Involvement of histone H1 in the organization of the nucleosome and of the salt-dependent superstructures of chromatin. J Cell Biol 83: 403–427
Thomas JO, Butler PJG (1980) Size-dependence of a stable higher-order structure of chromatin. J Mol Biol 144:89–93
Wang JC (1974) Unwinding of DNA by actinomycin D binding. J Mol Biol 89:783–801
Wilkins MHF, Zubay G, Wilson HR (1959) X-ray diffraction studies of the molecular structure of nucleohistones and chromosomes. J Mol Biol 1:179–185
Zamenhoff S (1957) Preparation and assay of deoxyribonucleic acid from animal tissue. Methods enzymol 3:696–671